An Assessment of Radiation Models Utilized in CFD for Thermal and Fluid Analysis in Interior Building Spaces with Large Glazing

Yona Arike Samuel [a)], Thomas Confrey [b)], Ashish Vashishtha, Dean Callaghan, and Cathal Nolan

South East Technological University, Carlow, Ireland

[a)] Corresponding author: yona.samuel@itcarlow.ie
[b)] thomas.confrey@itcarlow.ie

Abstract. This paper investigates the effects of using the S2S and the DO method in the CFD simulation of a cavity to identify a convenient model for simulating radiative heat transfer. A 3D model for an office room fitted with a sizeable controllable glass window was developed to carry out a transient analysis of a room's thermal performance when the glass is at its opaque state while accounting for each of the models. A transient user-defined function (UDF) boundary condition, based on radiative heat flux, was set as an incident solar load boundary condition on the dynamic glazing to study the dispersed temperature and the airflow in the room. Various configurations of the enclosed room with initial wall boundary condition and airflow in the room were considered under the effects of different parameters such as thermal properties, Rayleigh (Ra) and Grashof (Gr) numbers, surface emissivity, and absorption. Radiative CFD results were compared, and the importance of accounting for radiation was noted. The S2S displayed good performance, whereas unexpected temperature distribution was observed with the DO method. Although heat transfer depends on the transmitting material's thermal properties, further analysis has shown that the S2S, along with the SST k-ω viscous turbulence model, using piecewise linear approximation, is a reliable CFD model setting for performing a thermal analysis of a highly glazed enclosed room. The results were also compared to a previous 2D analysis of an enclosed space without accounting for radiation. Results had shown that the interior temperature was less than 2% for the S2S when radiation was overlooked. Further study would involve the validation of the computed room temperature with experimental data which will show the efficiency of the two radiation model methods in performing the thermal performance of a building.
.

Keywords: Solar radiation, CFD, smart glazing, 3D simulation, heat transfer.

INTRODUCTION

Solar radiation is a significant factor in a highly glazed room space where the incident heat passes through the transparent glass, thus heating the room. As a result, the room interior becomes overheated due to solar gain, creating an uncomfortable environment for residents. Smart controllable glass is one of the control measures used to control or mitigate solar heat gain [1]. When investigating the thermal behavior of a naturally ventilated building, the thermal and fluid flow behavior prediction becomes challenging, especially when considering natural convection in an enclosure due to the difference in flow type formation in internal convection. Research has clarified the significance of accounting for radiation when modeling airflow, particularly regarding the air temperature profile in a naturally ventilated building. Radiation is generally accounted for when there is a difference in two nearby surfaces. The concept of heat transfer through natural convection and solar radiation in an enclosed space or building has been the subject of increased research in recent years [2]–[4]. It has undergone intensive experimental and numerical investigative analysis in many engineering applications [5]–[8]. In Computational Fluid Dynamics (CFD) simulation, the effect of radiative heat transfer is often neglected because most engineering problems are dominated by a high rate of convective heat transfer. Including radiation heat transfer can be computationally expensive due to the higher order of the temperature involvement, which requires a considerable amount of computer resources. However, there are several important categories of problems where radiation heat transfer is highly important. Many researchers have proven that ignoring the radiation in thermal analysis of a building does not provide a realistic representation of the building heat transfer physics [9]. A naturally ventilated building space is one of the areas where modeling radiative heat transfer is highly necessary to predict a realistic thermal state. In these cases, the radiative heat flux is modest and comparable

with convective heat flux because the temperature variation is low in a room setting and buoyancy-driven flows often have small velocities [10], [11].

Meanwhile, the radiative heat flux is a function of temperature, material that has a high temperature emits more radiation than materials that have a low temperature. Therefore, as there is no direct coupling between radiation and the airflow field, the fluids' radiation properties and boundaries do not depend on the fluid flow velocity [12], [13]. The airflow field influences the spatial distribution of temperature, determining the intensity of the solar radiation emitted from boundary surfaces. Understanding these phenomena is vital for engineers and architects in designing low energy consuming buildings [14].

Researchers have employed many numerical and experimental methods of analyzing thermal performance while accounting for the effect of radiation [15]. CFD simulation is a well-known numerical method for producing accurate predictions of the combination of radiation and natural convection heat transfer in a building [8]. The calculation of the natural convection and radiative heat transfer has been challenging and resource-intensive due to the development of algorithms that compute the radiation intensity as a function of the position, angular direction, and radiation wavelengths in the computational domain. Over the years, many CFD methods have been developed for calculating the radiative heat transfer, which includes various analytical approximation techniques and groups of numerical methods. These methods include the Monte Carlo (MC), P-1, Rosseland, Discrete Ordinates (DO), Discrete Transfer (DT), and surface-to-surface (S2S) radiation models. Each has different ways of treating angular dependence and spatial variation intensities. The way of choosing a suitable model for thermal analysis in a building setting depends on the optical thickness of the quiescent fluid in the room or whether or not the fluid participates in the absorption of solar radiative heat transfer [16].

A fundamental numerical study on the combination of natural convection and radiation heat transfer of various anisotropic absorbing emitting scattering media in a 2D square cavity, based on the DO and the Boussinesq approximation method was studied by Liu, Gong, and Cheng [17]. Rayleigh number, optical thickness, scattering ratio, scattering phase function, and the aspect ratio of the square on heat transfer behavior were all explored. Their results have indicated that when the optical thickness increases, the radiation Nusselt number along the wall decreases. Similarly, Zhou et al. [12] analyzed combined natural convection and radiation heat transfer in a partitioned rectangular enclosure with semitransparent walls. Two types of boundaries were considered, one with an isothermal process on an opaque wall and another with an incidence of a constant radiation heat flux on the semitransparent wall. The turbulence renormalization group (RNG) k-ε model and the DO model were used to compute the radiation/natural convection heat transfer. Results show that the semitransparent wall facilitated reduced heat losses and obtained a higher temperature distribution compared to the opaque wall. Ababsa and Bougoul [18] presented a numerical analysis of a natural convection and radiation heat transfer in an inclined thermosiphon installed in the roof of a building where the Boussinesq approximation was utilized. Due to the channel's flow being turbulent, the k-ε epsilon model was used with the DO-model for the radiation. On the other hand, Cook, Zitzmann [19] showed a dynamic thermal building analysis with CFD radiation modeling, where the Monte Carlo (MC) and the Discrete Transfer (DT) radiation models were investigated, and both the results were compared. The DT mode gave an excellent performance in the simulation, whereas an unrealistic radiation distribution was observed with the MC on the surface domain. Zitzmann [20] performed a comparative study on the MC and the DT models in adaptive modeling of dynamic conjugate heat transfer and air movement using CFD. These results displayed a similar conclusion as analyses in [19], where the MC model revealed the unrealistic spatial distribution of radiative heat transfer. As a result, Zitzmann [20] proceeded with the DT model to analyze the dynamic thermal physics of the building. Menchaca-Brandan et al. [21] looked closer to the influence of radiation heat transfer on predicting airflows in rooms under natural convection when heated with and without radiation. The surface-to-surface (S2S) radiation model in CFD, while accounting for the emissivity of a black body surface and an assumed airflow in the room, is transparent to radiation. Their results disclosed a significant difference in accounting for radiation and when radiation was ignored. The results had shown that the internal temperature of the airflow when the effect of radiation was ignored was lower by 2°C – 4 °C relative to when radiation is accounted for. Voeltzel, Carrié, and Guarracino [9] studied the thermal and ventilation modeling of large, highly glazed spaces. They adapted AIRGLAZE as a new model that employed the S2S radiation model to improve the prediction of the large, glazed spaces' thermal behaviors. Lloyd [11] adapted the P-1 radiation model to determine the natural convection and radiation heat transfer in a small enclosure with a non-attached obstruction. The author's simulation was conducted with a ranging temperature of between 310k and 1275k that was imposed on the boundary conditions. Risberg [22] also used the P-1 radiation model for a CFD simulation and evaluated the different heating systems installed in a low energy building, located in a sub-arctic climate, where the influence of buoyancy was analyzed using Boussinesq approximation. He found that only a floor heating system could achieve a desired thermal

indoor environment in a low energy building. In another investigation of thermal indoor climate for passive housing in the same region of the sub-arctic area, Risberg used the DT radiation model with an emissivity of 0.9 for the opaque wall surfaces and 0.83 emissivity for the glass windows. A heat flux boundary condition in a steady-state simulation was used to study the room's thermal behavior as the wall and glass was heated up.

The Radiation models

Factors such as the optical thickness, the scattering, emissivity, particulate effects, the enclosure radiative heat transfer with no participating media, etc., play a significant role in deciding which radiation model to be used for a thermal analytical problem of a building [16]. Liu et al. [17] completed an intensive calculation to obtain the ideal optical thickness of a square cavity to select the DO radiation method for analyzing the thermal behavior of the cavity. The DO model solves the radiative transfer equation for a finite number of discrete solid angles associated with a vector direction in the global Cartesian system [10]. Compared to the DT, the DO model cannot perform ray tracing but transforms the transport equation for the allocated coordinates' radiation intensity [18]. The transport equation is solved for as many as specified directions. The solution method for the DO is similar to solving the fluid flow energy equations [14]. CFD has two energy implementations of the DO model, which include the uncoupled and coupled. The uncoupled is sequential and uses a conservative variant of the finite volume scheme, an extension to an unstructured mesh. Simultaneously, the energy equations and radiation intensities for the uncoupled are solved one by one, assuming a universal value for the other variables such as the thermal conductivity, viscosity and the scattering ecoefficiency [16]. In the coupled ordinate method, the energy and intensity equations were solved simultaneously at each cell. It is advantageous to use the coupling method to speed up the calculation for the applications involving high optical thickness and high scattering coefficients. This method also significantly improves the convergence in those applications that have more than 10 optical thickness.

The surface-to-surface radiation model is used to model radiation exchange in an enclosure of diffused gray surfaces. The energy exchange between two bodies depends on the sizes, distances, and orientation [16], which are accounted for using a view factor. Since the emissivity and the absorptivity of a gray surface are independent of the wavelength, the S2S permits absorption, emission, and scattering of radiation to be overlooked. It uses Kirchhoff's theory of radiation and absorption ($\varepsilon = \alpha$) [23]. As in most applications, the S2S model is applied on an opaque surface, which means that the transmissivity can be ignored as presented by the conservation of energy equation [24]. Energy flux leaving a given surface is composed of direct emitted (incident) and reflected energy. The reflected energy flux depends on the incident energy flux from the surroundings, expressed in terms of the energy flux leaving other surfaces. The S2S radiation model is well-known for modeling a radiation heat transfer in an enclosure without participating media. Compared to the other models, the advantage that the S2S holds is that it assumes that the incident radiation is diffused when modeling heat transfer in an enclosure, which means that it does not consider the incident radiation angle [16]. It treats all the radiation on the surfaces as isotropic intensity [25]. It does not account for participating media when modeling radiative heat transfer, and it has a much faster time per iteration than other radiation models.

Objective

A comprehensive review of numerical 2D CFD models of a turbulence natural convection heat transfer in a rectangular enclosure using experimental and numerical approach was carried out by Wood et al. [26], who concluded that the 2D analysis only displays a partial representation of the real physics with the analyzed enclosed system. Consequently, there is a need to investigate the effects of the thermal and fluid flow properties in buildings, considering natural convection and solar radiative heat transfer in 3D sets, to understand the application of the results to real-world cases. Although the radiation models such as the DO and the S2S are preferred for solar radiation heat transfer in building settings, accounting for solar radiation significantly affects the thermal performance of the building. Simulating the thermal condition requires defining the material types used and their properties to obtain a realistic result when using CFD simulation. This paper looks at a 3D assessment of the S2S, and the DO radiation models utilized in CFD for thermal and fluid analysis in interior building spaces with extensive smart glazing. The study draws a broader understanding of the performance of each model in participating in the heat transfer that involves natural convection and radiation and leads to a closer investigation of the occupants' thermal comfort in such a highly glazed environment as well as the benefit of using smart glass windows to control the overheating of rooms due to the solar heat gain.

MODELING APPROACH

In this study, a 3D enclosure, as shown in **Fig 1,** is considered with a large smart glass surface. A transient thermal physical analysis was performed to assess the effect of the CFD radiation models. The simulation setting followed a previous study on the analysis of thermal and fluid flow physics in building utilizing smart glazing to mitigate solar gain in an office room [1], with the heat sources obtained from experimental data on a smart glass test cell in its opaque state as performed by Ghosh et al. [27]. This study was based on a ground floor office room located in the Institute of Technology Carlow, Ireland, to create the 3D domain building stratification in ANSYS 19.1 design modular of the radiation model assessment. Boundary conditions were used to identify the walls and defined using the thermal condition's physical properties. The wall thickness was considered as a zero-wall thickness, with the smart window having an emissivity (ε) of 1 to develop a benchmark to a realistic analysis where the wall and glass thickness would be accounted for [28], [29]. The enclosed room had a length of 7.2 m, a width of 6.5 m, and a height of 3.6 m. The Sidewalls, floor, and ceiling were considered adiabatic walls, while the front wall was assigned a constant room temperature of 293.15K, and the smart window was defined as the heat source.

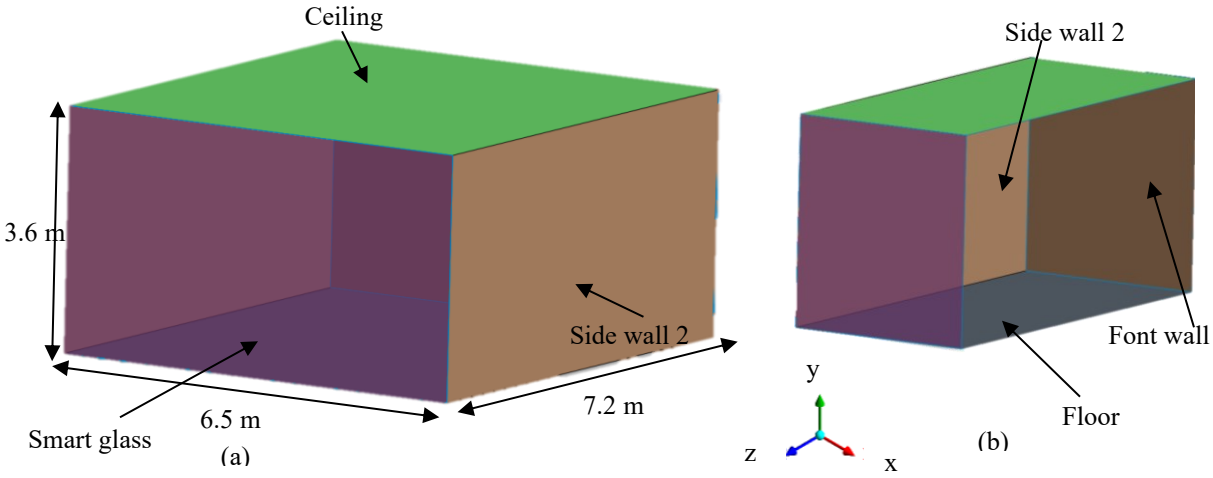

FIGURE 1. (a) Schematic CFD domain of enclosure, describing boundary conditions and (b) the cross section of the enclosure showing boundaries that is concealed in (a).

A structured mesh with a hexahedral element and an element size of 0.1 m was applied in the 3D domain with a fine near-wall mesh and a face mesh application for better convergence and high resolution to capture all the convective radioactive surface heat transfer and fluid flow in the boundary layers of the domain. The governing equations for a fluid flow and radiative heat transfer for natural convection and radiation were the conservation of momentum, mass, and energy [10], [11]. These equations are coupled with supporting equations such as the radioactive heat transfer, density, and the view factor equations [10]. The analysis used the Cartesian coordinate system to analyze the assessment discretization process of the selected radiation methods. The identified radiation models in CFD were used in the model domain one after the other and analyzed using initial properties. The boundary condition model, settings of a previous study of a 2D domain are employed in this study [1]. However, a transient boundary condition of the heated window is considered. The front wall was considered an isothermal wall exposed to an initial ambient room temperature of 293.15 K. The other walls were deemed to be adiabatic walls. Since the study focuses on the coupled system of both natural convection and radiation, the simulation was carried out with a coupled pressure based CFD algorithm for a robust and efficient single-phase implementation of a transient flow. A higher discretization solution method was chosen to minimize the occurrence of errors. A lower value time step of 0.1 was used to reach a converged solution of the transient simulation for one hour. The simulation was considered converged when the convergence criteria of the root mean square residual (RMS) for continuity, momentum and energy of less than or equal to the recommended values of 1e-5 or 1e-6 residual were achieved [28].

The simulation was carried out for the two identified radiation methods, surface-to-surface (S2S) and the Discrete Ordinance (OD). A user-defined function (UDF) boundary condition based on time-dependent radiative heat flux was set as an incident solar load boundary condition on the glazing. It is to monitor the effect of the ambient temperature and the airflow as the boundary heat flux increases over time. This is set to determine a suitable radiation model

between the identified modes that could be used for a further study to determine the thermal performance of the office room when installed with smart glazing and regular glazing. This was done when the extensive glazing was considered as opaque (black surface) to represent the smart glazing. It was set to monitor the dispersed temperature and the airflow due to the buoyancy effect in the enclosure interior.

Boundary condition

Various configurations of the enclosed room with the initial interior temperature and fluid flow boundary condition in the room were considered under the effects of different parameters as shown in **Table 1,** such as thermal properties, Rayleigh (R_a), and Grashof (G_r) numbers, Prandtl number (P_r), surface emissivity, absorption. A variation of the air density as a function of temperature gradient was included by considering a piecewise linear approximation. The SST k-ω turbulence model was also considered due to the size and nature of the airflow in the room, which resulted from other calculated air properties. The operating condition was set to an atmospheric condition. The thermal properties of the room were calculated using the formulae below [17].

$$R_a = G_r . P_r = \frac{g\beta(T_{wall} - T_\infty)L^3}{\nu\alpha} \tag{1}$$

Where Ra is the Rayleigh number, Gr is the Grashof, P_r is the Prandtl number, g is the acceleration due to gravity (-9.81 m/s^2), β is the coefficient of thermal expansion, T_{wall} is the temperature of the wall, T_∞ Is the bulk temperature, L is the vertical length, and ν is the kinematic viscosity, and α is the thermal diffusivity (m^2/s). For gases (air), β = 1/T, where the temperature is measured in Kelvin (K).

$$G_r = \frac{g\beta(T_{wall} - T_\infty)L^3}{\nu^2} \tag{2}$$

$$P_r = \frac{\nu}{\alpha} = \frac{\frac{\mu}{\rho}}{\frac{k}{\frac{C_p}{\rho}}} = \frac{\mu . C_p}{k} \tag{3}$$

The α is the thermal diffusivity (m^2/s), μ is the dynamic viscosity (Ns/m^2), and k is the thermal conductivity (W/mk), C_p is the specific heat (J/kgk), while ρ is the fluid density (kg/m^3). Small values of Prandtl number i.e. $P_r <$ 1, the thermal diffusivity dominates, whereas the larger the Prandtl number i.e. $P_r >$ 1, the momentum diffusivity dominates.

TABLE 1. Calculated natural convection properties

Wall Temperature (T_{wall}) (K)	Prandtl number (P_r)	Grashof number (G_r)	Rayleigh number (R_a)
293.15	0.726	0	0
303.15	0.76	543.473×10^9	461.952×10^9
313.15	0.726	1086.947×10^9	923.905×10^9
323.15	0.726	1630.419×10^9	1389.857×10^9
333.15	0.726	2173.893×10^9	1847.809×10^9

Grid independence test

With the use of the structured mesh type, a grid independence test was performed with various element size and edge sizing while keeping a constant bias factor to achieve an acceptable mesh size that would have minimum results variation. Since small changes in results during any CFD study is impossible to avoid [30], to capture all the information (temperature and airflow) and to minimize the discretization errors, a bias factor of 5 was introduced in the edge sizing to create a refinement along the walls while keeping the center with a coarser grid. The simulated grid sizes were chosen so that minimal (almost constant) values in the results would be identified to proceed with the simulation for the chosen duration.

TABLE 2. Grid independence study

Grid (G)	Name	Mesh element size (m)	Bias-factor	Mesh element
G1	Coarse	0.20	0.5	23199
G2	Medium	0.15	0.5	53900
G3	Fine	0.10	0.5	178266

The grid independence studies were performed for the 3D domain to monitor the temperature and the airflow for different mesh element with different edge sizing. A piecewise linear function, the shear stress transport (SST) k-ω turbulence model, second discretization method and a constant heat flux of 60.13 W/m^2 were used so that a suitable grid could be obtained for the two radiation model studies. Transient temperature and airflow were monitored at the ZY center-line of the room interior. Among the coarse, medium and fine grids, small variation of less than 1% is observed between medium (G2) and fine (G3) grid for the temperature and airflow as shown in **Fig. 2**. The three solutions are obtained by using same time-step interval. The temporal fluctuations in air flow are slightly deviates for coarse grid, however the medium and fine grids show similar trend with least variation. The medium grid (G2) was further selected to assess the two-radiation model since it displays a grid-independent solution.

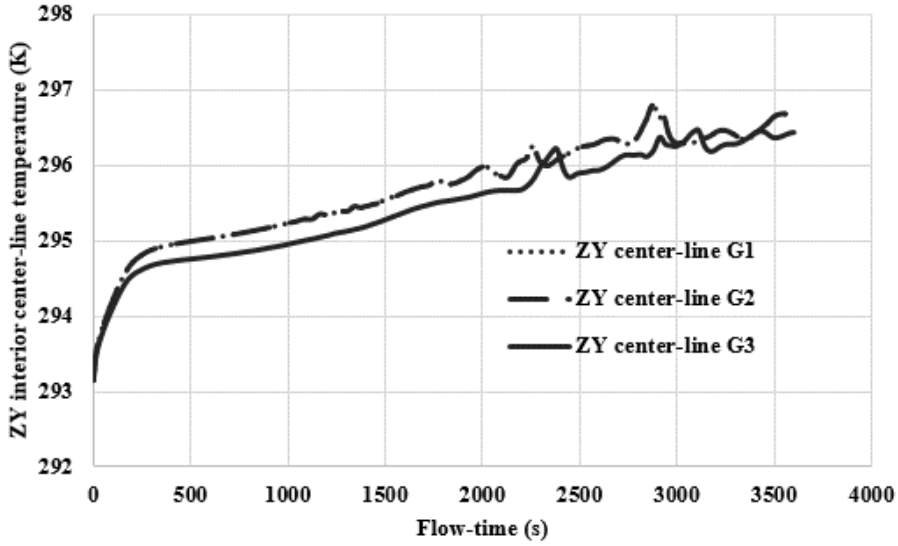

FIGURE 2. Grid independent study of temperature distribution

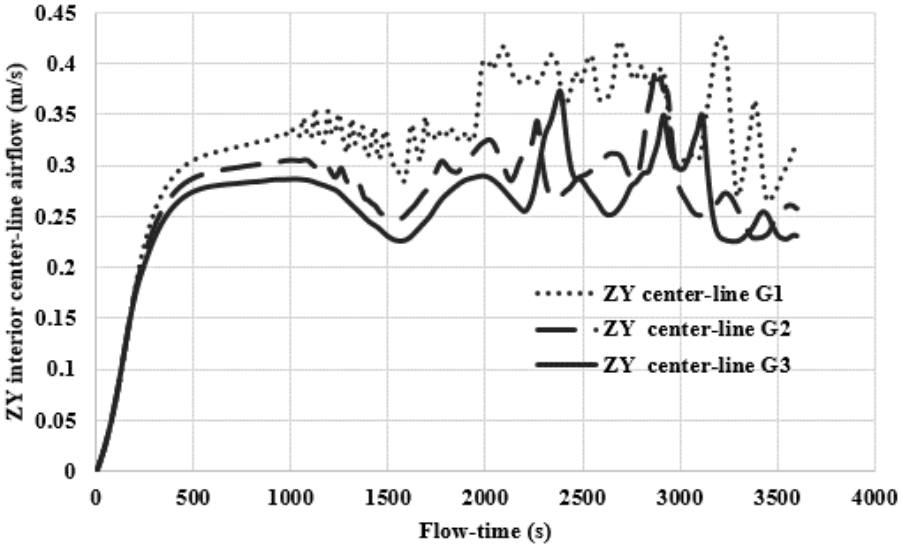

FIGURE 3. Airflow of the analysed the domain.

Radiative Heat flux boundary heat source

This study aimed to evaluate the effect of the two identified radiation models based on the optical thickness, the scattering emissivity, particulate effect, as specified in the ANSYS theory guide [16]. The simulation was performed in two cases where Case A1 is with the S2S radiation model, and Case A2 is with the DO radiation model, as seen in **Table 2**. Since the heat source is considered a black-body surface, the thermal properties of a black-body surface were well-defined where the radiative heat flux is defined by the equations below, and values are equated in **Table 3** and **Table 4** below. The heat flux on the glazing is set as time-dependent to monitor the effect of the ambient temperature and the airflow as the boundary heat flux increases over time. This is set to determine a suitable radiation model between the identified modes that could be used for a further study to determine the thermal performance of the office room when installed with smart glazing and regular glazing. The black-body surface is regarded as an ideal surface that has a perfect absorption of all radiation subjected to it regardless of the direction of the wavelength [31]. The surface had a property of 0 reflectivity (ρ) and 0 transmissivities (τ), and 1 emissivity (ε), as described in **Table 5**.

TABLE 3. Investigated radiation models for the enclosed room

Evaluated cases	Radiation model
A1	Surface to Surface (S2S)
A2	Discrete Ordinates (DO)

TABLE 4. Boundary conditions

Boundary Condition	Type	Thermal property	Temperature
Ceiling	Wall	Adiabatic	0
Floor	Wall	Adiabatic	0
Sidewall 1	Wall	Adiabatic	0
Sidewall 2	Wall	Adiabatic	0
Front wall	Wall	Adiabatic	0
Smart window	Wall	Heat source	UDF transient heat flux

TABLE 5. Calculated transient UDF heat flux boundary condition subjected to the smart glass window, including the time steps.

Flow time (s)	Heat flux (W/m^2)
0	60.13
1200	60.13
2400	102.053
3600	117.555

TABLE 6. Surface properties in a radiative heat transfer.

	Absorptivity (α)	Reflectivity (ρ)	Transmissivity (τ)	Emissivity (ε)	Scattering (σ_s)
Perfect absorption	1	0	0	0 - 1	0 - 1
Perfect reflection	0	1	0	0 - 1	0 - 1
Perfect transmissivity	0	0	1	0 - 1	0 - 1
Black-body	1	0	0	1	0
Grey-body	0 - 1	0 - 1	0 - 1	0 - 1	0 - 1

$$Q_{rad} = \varepsilon\sigma(T_S^4 - T_\infty^4) \tag{4}$$

Where Q_{rad} is the radiative heat flux, ε is the surface emissivity ($\varepsilon = 1$ for a black body), is the σ is the Stefan Boltzmann's constants ($\sigma = 5.6704 \times 10^{-8}$), A is the surface area, $T_{surface}$ is the surface temperature.

The assessed model uses the fundamental Radiation Transport Equation (RTE) for the finite number of discrete solid angles. Each associated with a vector direction is fixed in the global Cartesian system [10]. Each model is defined by a unique equation as described below. However, CFD uses RTE to simulate solar radiation cases [16].

$$\frac{dI(\vec{r},\ \vec{s})}{ds} + (a + \sigma_s)I(\vec{r},\vec{s}) = an^2\ \frac{\sigma T^4}{\pi} + \frac{\sigma_s}{4\pi}\int_0^{4\pi} I(\vec{r},\qquad \vec{s})\Phi\left(\vec{s}.\overrightarrow{s^t}\right)d\Omega^t \tag{5}$$

Where $\vec{r}$ and $\vec{s}$ are the position and direction vectors, respectively, $\overrightarrow{s^t}$ is the scattering direction vector, s is the path lengths, a is the absorption coefficient, n is the refractive index, σ_s is the scattering coefficient, σ is the Stefan-Boltzmann constant (5.669 × 10-8 W/m^2-k^4), I is the radiation intensity, T is the local temperature, Φ is the phase function, and Ω^t is the solid angle.

Discrete Ordinates (DO)

The DO solution is equated in the discrete transfer model by discretizing the computational radiation domain into homogeneous surface and volume elements. The rays are emitted from the center of each boundary surface element with each position vector in the direction determined by discretizing solid hemispherical angle above the surface into finite solid angles. In calculating the solid angle element to the incident at the origin, the intensity distribution along its path is solved with the recurrence relation.

$$I_{n+1} = I_n e^{-\beta\delta_s} + S(1 + e^{-\beta\delta_s}) \tag{6}$$

Where n and n+1 designate successive boundary, locations separated by a distance δ_s when the ray passes through each surface control volume. The source function S includes the scattering integral in its angular discretized form see [10].

$$S_i = (1 - \omega)\mathrm{I_b} + \frac{\omega}{4\pi}\sum_{j=1}^{n} wI\Phi \tag{7}$$

Surface to Surface (S2S)

For the S2S model, the heat flux leaving a specified surface is composed of directly emitted and reflected heat energy. The reflected heat energy is dependent on the incident solar energy flux from the surroundings. Therefore, it is expressed in terms of the heat energy leaving from the other surfaces. The reflected energy from a specified smart glass can be expressed as:

$$\mathrm{q_{out}} = \in_m \sigma \mathrm{T_s^4} + \rho_\mathrm{s} \mathrm{q_{in,s}} \tag{8}$$

Where $q_{out,sg}$is the solar heat energy flux leaving the smart glass surface, $\in_{sg}$ is the emissivity, σ is the Stefan Boltzmann's constant, and the $q_{in,sg}$ is the incident heat energy flux on the surface from the surrounding areas.

Due to the radiation being transmitted from S2S, the total heat energy upon a surface from another surface is a direct function of the S2S view factor (F). The view factor is the fraction of heat energy leaving the surface (s) that is incident to the front surface.

The solar heat flux q_{in} from the smart glass is expressed in terms of the heat flux leaving the surface as:

$$\mathrm{Aq_{in}} = \sum_{surface=1}^{N} Aq_{out}F \tag{9}$$

Where A is the area of the smart glass, F is the view factor between the smart glass and the incident front wall surface. The N surface uses the view factor reciprocity relationship, which gives:

$$\mathrm{A_w F} = \mathrm{A_s F} \tag{10}$$

Therefore,

$$\mathrm{q_{out}} = \in_\mathrm{s} \sigma \mathrm{T_s^4} + \rho_{glass} \sum_{\mathrm{fw}=1}^{\mathrm{N}} \mathrm{F q_{out,}} \tag{11}$$

CFD generates the view factor for all the surfaces by applying these equations to all the walls during a simulation.

ASSESSMENT OF RESULTS

This paper describes a 3D assessment of radiation models utilized in CFD for thermal and fluid analysis in interior building spaces with large smart glazing. The aim was to draw a broader understanding of the performance of each of the identified models to develop a robust CFD radiation model that would be used to examine occupants' thermal comfort in an office environment, thereby obtaining a better knowledge of the benefits of utilizing the smart glazed windows to control the solar heat gain. Two CFD radiation methods were investigated in terms of their radiative heat transfer considering natural convection in a room with a large smart glass window. Parameters such as temperature and airflow were monitored for each of the models as the room domain was simulated for 12000 seconds.

The results for each case presented are compared through temperature and airflow contour plots along a vertical plane (Z-Y) created in the middle of the 3D office room. The Z-Y middle plane was used to illustrate the differences in the interior temperature distribution and the airflow. The obtained results were due to the transient heat flux that was exposed to the window. The exposed solar heat flux was calculated using Stefan's Boltzmann law of radiative heat flux of a black body due to its temperature as described by equation **(4)**. The boundary condition was based on the previous CFD numerical analysis that used constant temperature as a boundary condition to account for the thermal condition of the room. Although the previous studies were based on natural convection (buoyancy effect), they did not consider the effect of radiation. A broader insight into the performance of each radiation model is depicted as the CFD settings remain the same except for the radiation methods.

Figure 6 and **Fig 9** describe the contour plots of (a) the temperature distribution and (b) the airflow at the Z-Y center plane of the 3D enclosed domain. In contrast, **Fig 3** and **Fig 5** provide a graphical representation of the maximum recorded interior (a) temperature and (b) air velocities for the 2D Z-Y median plane of the 3D domain. Temperature and airflow differences were observed from the analyzed results. The figures below describe each of the models and present a comparison of each simulated outcome. The results were also compared with existing literature in similar area to provide an ideal radiation model for further research. The results have indicated a buoyancy-driven recirculating of air as the glass was being heated, contributing to the mixing of the air within the enclosed. Thus, the effect of natural convection was witnessed in previous 2D research analyses [1].

Case A1: Temperature distribution and airflow using the surface-to-surface model

Error! Reference source not found. and **Fig 5** and **Fig 6** displayed an excess temperature and airflow respectively of the S2S model compared to the rest of the analyzed system. The entire 2D domain was observed to have an average interior temperature of about 308.29 K and an average interior airflow of more than 0.0713 m/s, respectively. In comparison, the contour results on the Z-Y middle plane displayed an identical average interior temperature to the interior temperature distribution, and airflow of 0.081 m/s as the window temperature ranges from 293.15 K to an average temperature of 323.25 K. These temperatures are too hot for a normal room temperature. However, for study purpose, the study aims to assess the two-radiation model. It does not consider occupants in the room. This result is due to the subjection of a high boundary condition on the window using a UDF macro to determine the suitable radiation model that can be employed to study the thermal behavior of smart glazing in creating a comfortable living/working environment for people.

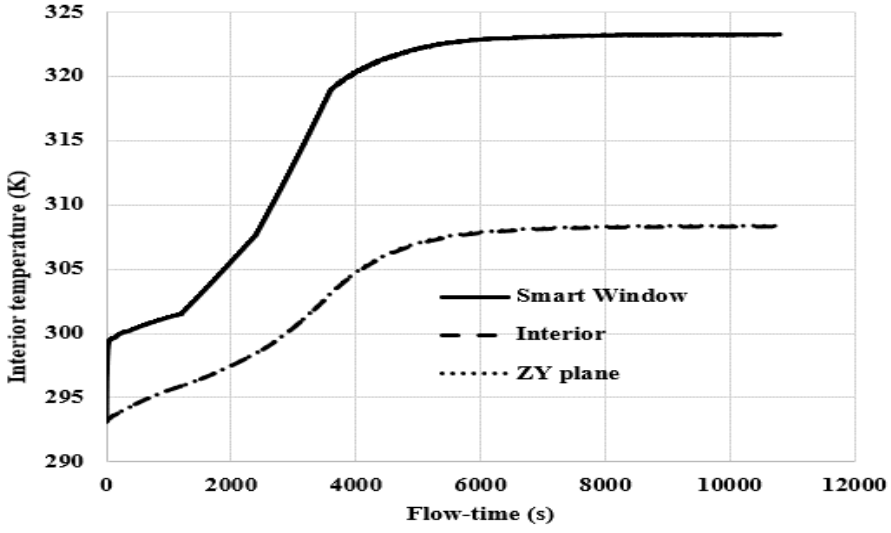

FIGURE 4. Interior temperature distribution

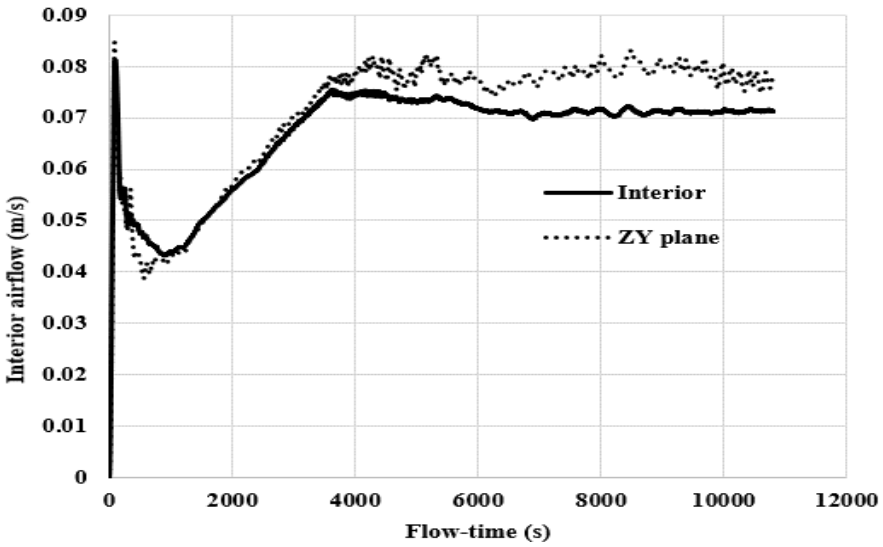

FIGURE 5. Interior airflow of the enclosure as a transient udf heat flux were used as a boundary condition on the smart glass using the S2S radiation model.

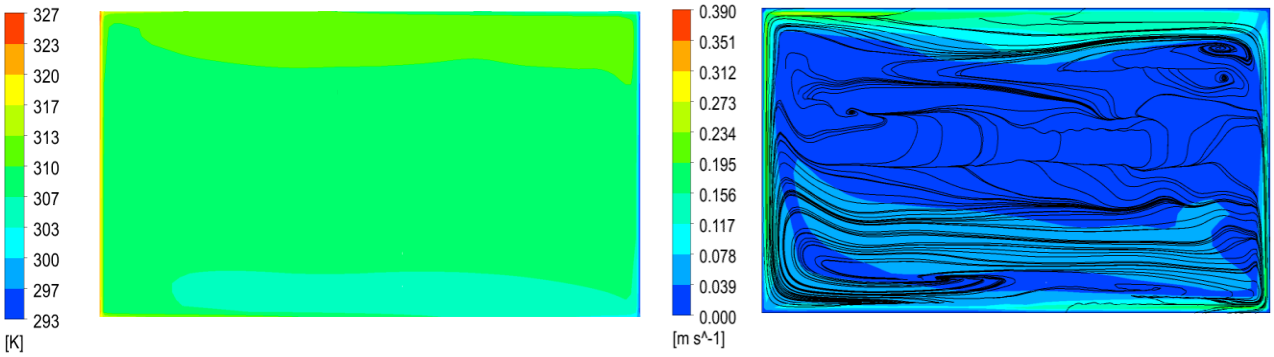

(a) (b)

FIGURE 6. A 2D representation of the Z-Y middle plane with (a) temperature distribution and (b) airflow in the enclosure for the S2S radiation model.

Case A2- Temperature distribution and airflow using the Discrete Ordinates

For the DO method, **Fig 7** and **Fig 8** and **Fig 9** illustrates the temperature and air velocity distribution in the Z-Y domain as the smart window temperature varies from 293.15 K to 323.89 K and an interior airflow of less than 1 m/s.

Figure 9 illustrates the 3D temperature and airflow of the domain, which is 308.88 K and 0.0795 m/s, which is higher than the results obtained from the S2S model.

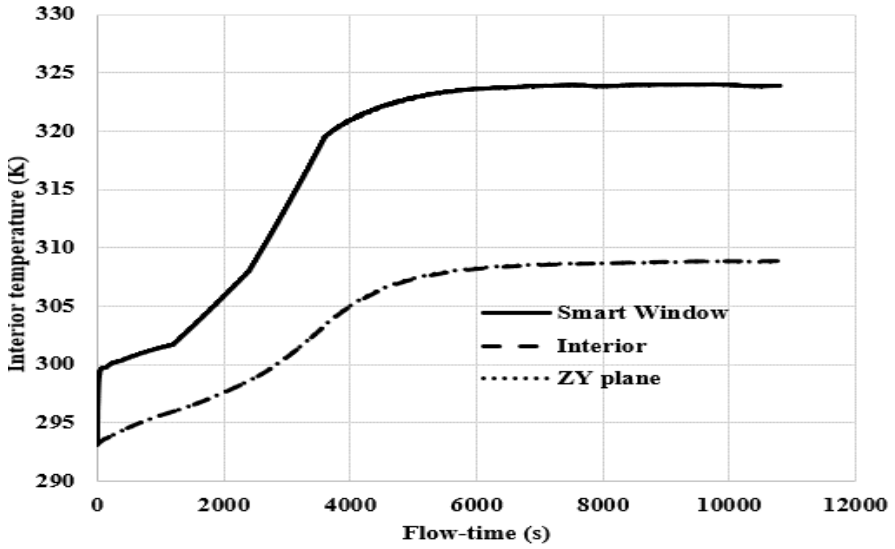

FIGURE 7. Interior temperature distribution

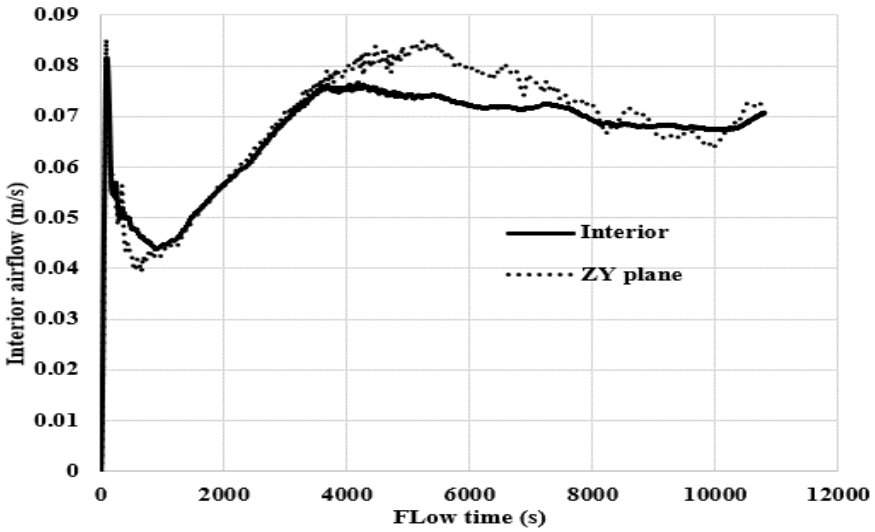

FIGURE 8. Interior airflow of the enclosure as a transient heat flux is used as a boundary condition on the glazing using the DO radiation model.

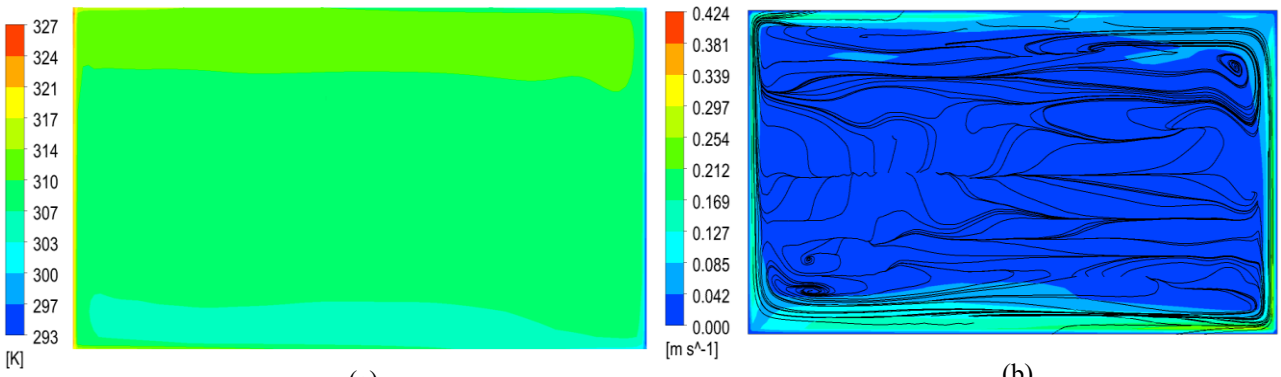

FIGURE 9. A 2D representation of the Z-Y middle plane with (a) temperature distribution and (b) airflow in the enclosure for the DO radiation model.

The temperature curve in **Fig 4** (a) and **Fig 6** (a) seems to be constantly increasing because of the increase in the heat flux boundary condition as time elapses. This is described by UDF boundary condition **Tab 4**. Since this was simulated for more than three hours (12000 seconds), it is observed that the simulation would require more time flow to reach a steady state.

DISCUSSION

As examined from previous research, radiation has a significant effect on the temperature distribution in a naturally ventilated enclosed and highly glazed space, which also has a high impact on the airflow in the enclosure [9], [10], [21]. When the obtained results of the two methods are compared to a previous investigation of a 2D enclosure without accounting for radiation [1], a significant difference is observed. The results have indicated that neglecting radiation in such studies would underpredict the temperature and airflow results in the enclosure. The predicted results would be lower than what they would have been. Therefore, the assessed model gives an understanding of the significance of radiation and how each model functions in terms of the air temperature and the airflow in a buoyancy-driven system. **Fig 7** shows the overall case-by-case examined smart glass facade and interior (a) temperature and each (b) interior air velocities. Thus, the difference between the two methods was observed.

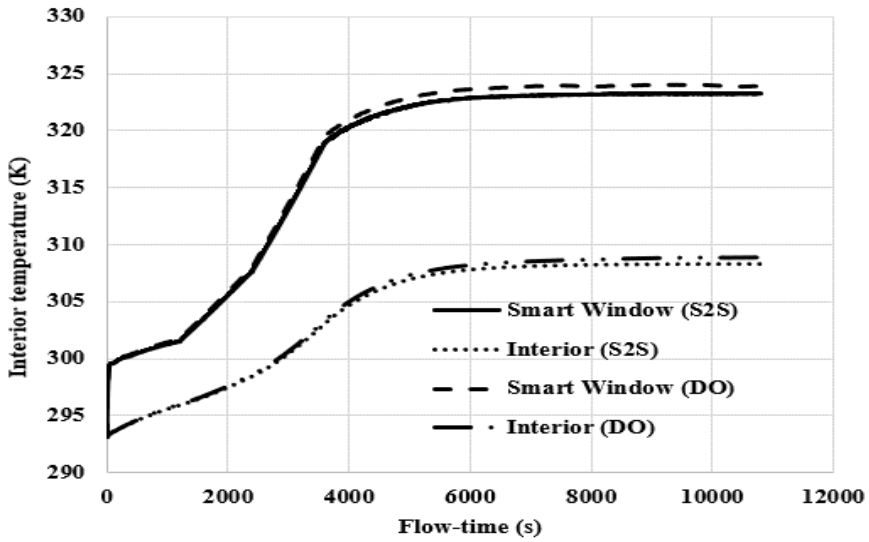

FIGURE 10. Showing the window temperature

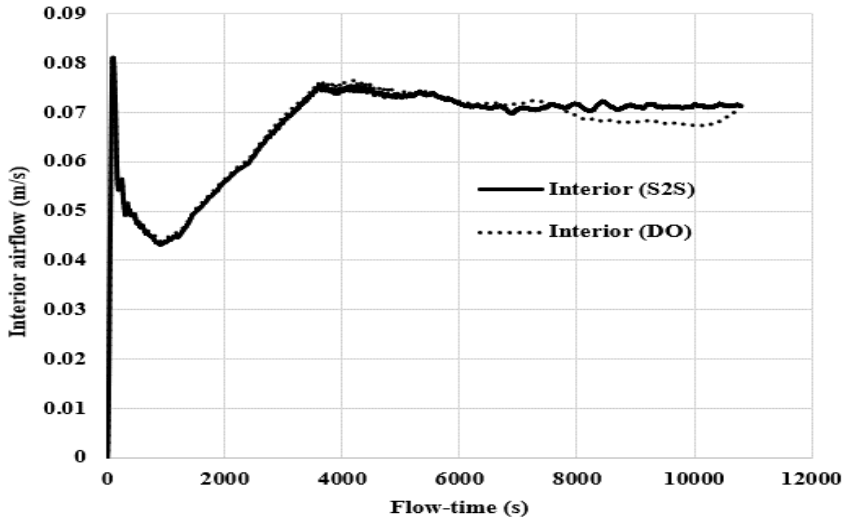

FIGURE 11. Interior airflow in the three-dimensional setting as transient radiative heat flux is exposed on the glass of each CFD radiation model.

FIGURE 11 shows the Z-Y middle plane with interior temperature distribution and air movement in the room. Since the S2S does not account for the absorption and scattering and the optical thickness, therefore, it displays the exact outcome of the radiative results of the temperature distribution in the cavity. Unlike the DO method, the results are lower for the smart glass temperature distinguishing from the S2S. This can be taken as due to the absorption and the scattering factor, which means that some radiative energies are absorbed in the system as described in equations (**6**) and (**7**). The CFD-used equation can be found in the works of H K Versteeg et al. [10].

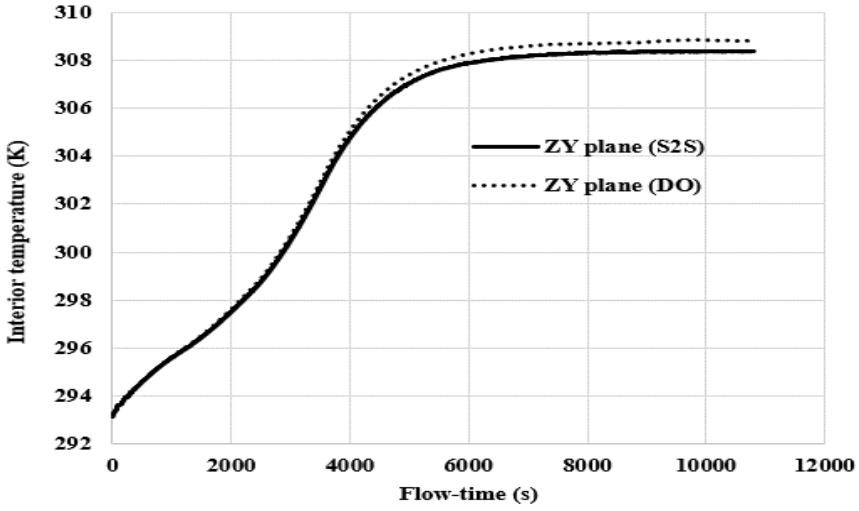

FIGURE 12. Case results of (a) Interior radiative temperature distribution

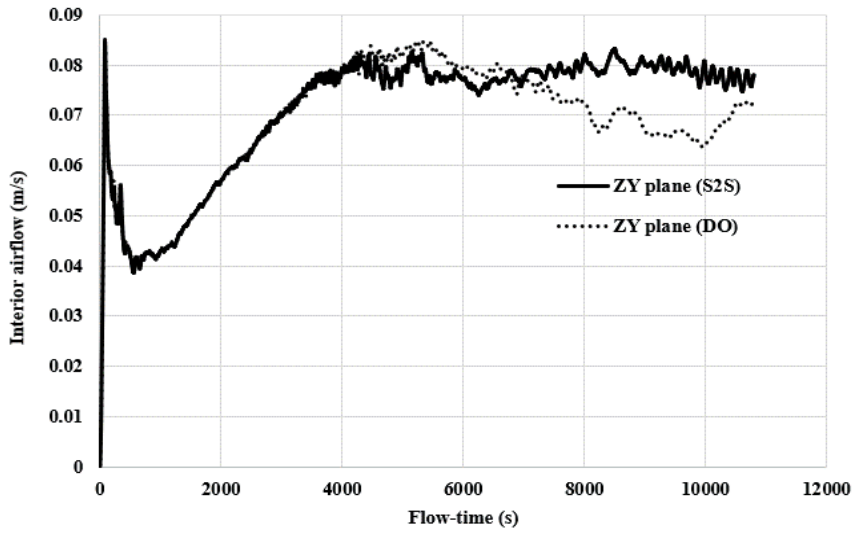

FIGURE 13. Interior airflow of the Z-Y 2D middle plane room when a transient radiative heat flux is exposed on the room wind.

As understood by the assessed models, examining the results obtained using the DO method in **Fig 10 a**nd **Fig 12,** it is seen that the interior temperature and airflow results have negligible difference in the results obtained using the S2S method in **Fig 4, Fig 5,** and **Fig 6**. Results are seen to agree with the works of Zhou et al. [12], where the temperature is evenly distributed in both analyses using semitransparent and opaque walls. However, the reliability of the results presented in [12] only applies to an enclosed system where the thickness of the boundaries of the domain are considered [17]. The obtained results of the current study are much higher than originally expected. During the simulation, it was observed that the DO requires a considerable amount of computer resources in solving the differential equation involved. However, they are suitable for a system with a defined thickness, absorption coefficient, emissivity values, scattering coefficients, and specified radiation intensity angle. The DO method would be best with a system where the gas participates in the process of radiation in which the gas absorbs and scatters some radiation [32].

For the S2S method, the results have a higher temperature distribution and a more increased airflow across the room than the DO process, as seen in **Fig 7** and **Fig 8**. The S2S method is used to model for radiation exchange in an enclosure of both a diffuse grey, opaque surface and the energy exchange between two surfaces, depending on the sizes, distances. This method allows absorption, emission, and scattering to be ignored, and only surface-to-surface radiation is considered. Menchaca-Brandan et al. [21] used this method where they found out that ignoring the radiation would reduce the interior temperature, which would indicate unrealistic results. Voeltzel et al. [9] also found that the S2S is a suitable method to account for radiation while ignoring the scattering, absorption, and emission from a black surface since a black-body is considered as a perfect reflector and absorber [33], [34]. Comparing the obtained results to the works of Menchaca-Brandan et al. [21], it is clear that temperatures are higher when radiation is included.

CONCLUSIONS

In this paper, a CFD numerical technique was developed for the transient simulation of a coupled natural convection and radiation for a stratified 3D enclosure with a large glazing window to assess the identified CFD radiation models' effect in a buoyancy-driven heat transfer system. The identified S2S and DO radiation methods were examined by monitoring the interior temperature distribution and the airflow of the room as transient UDF heat flux boundary condition was subjected to the glass window for each radiation method. The SST k-ω model was considered, including a piecewise linear approximation for the turbulent flow in the enclosure. Interior temperature and airflow of each case were compared to each other and to existing research to develop a reliable radiation model that would be employed to study the thermal comfort analysis of occupants in building fitted with smart glazing to control solar heat gain. Following the assessed cases, further research would be required to explore in more depth the aspects of

absorption, scattering, and optical thickness of the radiation domains using the DO method to draw a legitimate conclusion to the various elements of the CFD model. Most of the methods consider the trait of scattering, absorption, and emissivity when the walls are signed with thickness. With the simulated details and related literature, it is observed that the S2S, with the k-ω viscous turbulence model and using a piecewise linear approximation, the S2S is a reliable CFD model setting for performing a thermal analysis of a highly glazed enclosed room due to the immense heat flux and temperature variation [25]. The S2S also has a computational timing advantage over the other methods, which means that it does not require a considerable amount of computer resources. This can be used for a future study of the thermal comfort of occupants introducing passive ventilation and air condition systems installed with smart glass. This will indicate the difference between the ordinary glass windows and the intelligent glass windows in buildings to control the solar gain.

In future study, the computed room temperature will be validated with experimental measured data. This will show the efficiency of the two radiation model methods in performing the thermal performance and the thermal comfort of occupants in a building. Further assessment of the models using average values rather than maximum values would be much reasonable since the exact location of a particular maximum point is not known.

ACKNOWLEDGMENTS

Sincere thanks to the Teaching and Learning Centre at the Institute of Technology Carlow for their support in reviewing my research work. I would also like to acknowledge the financial support provided by President's Research Fellowship and the Dargan Center, Institute of Technology Carlow to carry out this research.

REFERENCES

[1] Y. Samuel, T. Confrey, D. Callaghan, N. Kent, and C. Nolan, "CFD analysis of thermal and flow physics in buildings utilizing smart glazing for mitigation of solar gain.," *Proc. Therm. Fluids Eng. Summer Conf.*, vol. 2020-April, pp. 151–161, 2020, doi: 10.1615/TFEC2020.ens.032102.

[2] N. L. Jones, I. Chaires, and A. Goehring, "Detailed Thermal Comfort Analysis from Preliminary to Final Design," *Proc. Build. Simul. 2019 16th Conf. IBPSA*, vol. 16, pp. 2675–2682, 2020, doi: 10.26868/25222708.2019.210875.

[3] T. Marzullo, M. M. Keane, M. Geron, and R. F. D. Monaghan, "A computational toolchain for the automatic generation of multiple Reduced-Order Models from CFD simulations," *Energy*, vol. 180, pp. 511–519, 2019, doi: 10.1016/j.energy.2019.05.094.

[4] Y. Zhang, L. Huang, and Y. Zhou, "Analysis of indoor thermal comfort of test model building installing double-glazed window with curtains based on CFD," in *Procedia Engineering*, 2015, vol. 121, pp. 1990–1997, doi: 10.1016/j.proeng.2015.09.197.

[5] G. Smith, A. Gentle, M. Arnold, and M. Cortie, "Nanophotonics-enabled smart windows, buildings and wearables," *Nanophotonics*, vol. 5, no. 1. Walter de Gruyter GmbH, pp. 55–73, Jun. 01, 2016, doi: 10.1515/nanoph-2016-0014.

[6] Y. Ajaji and P. André, "Thermal comfort and visual comfort in an office building equipped with smart electrochromic glazing: An experimental study," 2015, doi: 10.1016/j.egypro.2015.11.230.

[7] N. U. I. Galway, "Calibrated CFD simulation to evaluate thermal comfort in a highly-glazed naturally ventilated room Author (s) Hajdukiewicz , Magdelena ; Geron , M ; Keane , MM Publication Date Hajdukiewicz , M ; Geron , M ; Keane , MM (2013) ' Calibrated CFD si," 2013.

[8] M. Hajdukiewicz, M. Geron, and M. M. Keane, "Calibrated CFD simulation to evaluate thermal comfort in a highly-glazed naturally ventilated room," *Build. Environ.*, 2013, doi: 10.1016/j.buildenv.2013.08.020.

[9] A. Voeltzel, F. R. Carrié, and G. Guarracino, "Thermal and ventilation modelling of large highly-glazed spaces," *Energy Build.*, vol. 33, no. 2, pp. 121–132, 2001, doi: 10.1016/S0378-7788(00)00074-8.

[10] H K Versteeg and W. Malalasekera, *An Introduction to Parallel Computational Fluid Dynamics*, vol. 6, no. 4. 2007.

[11] J. L. Lloyd, "Natural convection and radiation heat transfer in small enclosures with a non-attached obstruction," no. December, 2003.

[12] L. Zhou, J. Liu, Q. Huang, and Y. Wang, "Analysis of Combined Natural Convection and Radiation Heat Transfer in a Partitioned Rectangular Enclosure with Semitransparent Walls," *Trans. Tianjin Univ.*, vol. 25,

no. 5, pp. 472–487, 2019, doi: 10.1007/s12209-019-00208-9.
[13] H. Ertürk and J. R. Howell, *Monte Carlo Methods for Radiative Transfer*. 2017.
[14] Y. Ji, "CFD modelling of natural convection in air cavities," *CFD Lett.*, vol. 6, no. 1, pp. 15–31, 2014.
[15] P. Riederer, "Thermal room modelling adapted to the test of hvac control systems," 2004. [Online]. Available: https://pastel.archives-ouvertes.fr/pastel-00000632.
[16] ANSYS, "ANSYS FLUENT 12.0 User's Guide," *Ansys - Fluent Manual*, 2009. https://www.afs.enea.it/project/neptunius/docs/fluent/html/ug/main_pre.htm (accessed Jan. 04, 2021).
[17] X. Liu, G. Gong, and H. Cheng, "Combined natural convection and radiation heat transfer of various absorbing-emitting-scattering media in a square cavity," *Adv. Mech. Eng.*, vol. 2014, 2014, doi: 10.1155/2014/403690.
[18] D. Ababsa and S. Bougoul, "Modeling of natural convection and radiative heat transfer in inclined thermosyphon system installed in the roof of a building," *Heat Transf. - Asian Res.*, vol. 46, no. 8, pp. 1148–1157, 2017, doi: 10.1002/htj.21266.
[19] M. J. Cook, T. Zitzmann, and P. Pfrommer, "Dynamic thermal building analysis with CFD – Modelling radiation," *J. Build. Perform. Simul.*, vol. 1, no. 2, pp. 117–131, 2008, doi: 10.1080/19401490802250421.
[20] T. Zitzmann, "Adaptive modelling of dynamic conjugate heat transfer and air movement using computational fluid dynamcs," no. May, 2007.
[21] M. A. Menchaca-Brandan, F. A. Dominguez Espinosa, and L. R. Glicksman, "The influence of radiation heat transfer on the prediction of air flows in rooms under natural ventilation," *Energy Build.*, vol. 138, pp. 530–538, 2017, doi: 10.1016/j.enbuild.2016.12.037.
[22] Daniel Risberg, "Analysis of the Thermal Indoor Climate with Computational Fluid Dynamics for Buildings in Sub-arctic Regions," *J. Chem. Inf. Model.*, vol. 53, no. 9, pp. 1689–1699, 2019.
[23] Frank P. Incropera, David P. Dewitt, Theodore L. Bergman, and Adrienne S. Lavine, *Fundamentals of Heat and Mass Transfer*. 2007.
[24] John D Anderson, "Computational Fluid Dynamics: Chapter 2: Governing Equations of Fluid Dynamics," *Comput. Fluid Dyn.*, pp. 15–51, 2009.
[25] Aidan Wimshurst, *How does the Surface-to-Surface (S2S) Radiation Model Work*. 2018.
[26] K. Wood, B. Whitney, J. Bjorkman, and M. Wolff, "Introduction to Monte Carlo radiation transfer," no. July, pp. 1–20, 2001, [Online]. Available: http://www.patarnott.com/pdf/MonteCarlo2.pdf.
[27] A. Ghosh, B. Norton, and A. Duffy, "Behaviour of a SPD switchable glazing in an outdoor test cell with heat removal under varying weather conditions," *Appl. Energy*, vol. 180, pp. 695–706, 2016, doi: 10.1016/j.apenergy.2016.08.029.
[28] K. Javad and G. Navid, "Thermal comfort investigation of stratified indoor environment in displacement ventilation: Climate-adaptive building with smart windows," *Sustain. Cities Soc.*, 2019, doi: 10.1016/j.scs.2018.11.029.
[29] H. Montazeri, K. U. Leuven, S. Gilani, H. Montazeri, and B. Blocken, "CFD simulation of temperature stratification for a building space: Validation and sensitivity analysis," 2013. [Online]. Available: https://www.researchgate.net/publication/258645059.
[30] D. Risberg, L. Westerlund, and J. G. I. Hellstrom, "Computational fluid dynamics simulation of indoor climate in low energy buildings computational set up," *Therm. Sci.*, vol. 21, no. 5, pp. 1985–1998, 2017, doi: 10.2298/TSCI150604167R.
[31] D. D. Ganji, Y. Sabzehmeidani, and A. Sedighiamiri, *Nonlinear systems in heat transfer: Mathematical modeling and analytical methods*. 2017.
[32] Aidan Wimshurst, *The Discrete Ordinates (DO) Radiation Model*. Youtube, 2020.
[33] H. Ye, X. Meng, and B. Xu, "Theoretical discussions of perfect window, ideal near infrared solar spectrum regulating window and current thermochromic window," *Energy Build.*, vol. 49, pp. 164–172, 2012, doi: 10.1016/j.enbuild.2012.02.011.
[34] P. M. Robitaille, "Kirchhoff Law of Thermal Emission: 150 Years," vol. 4, 2009, [Online]. Available: http://www.ptep-online.com/2009/PP-19-01.PDF.